frontiers | Frontiers in Analytical Science

TYPE Original Research
PUBLISHED 22 January 2025
DOI 10.3389/frans.2024.1506786

OPEN ACCESS

EDITED BY
Massoud Kaykhaii,
University of Tasmania, Australia

REVIEWED BY
Sangeetha Selvam,
University at Albany, United States
Joanna Zembrzuska,
Poznań University of Technology, Poland

*CORRESPONDENCE
Zhiqin Yuan,
yuanzq@mail.buct.edu.cn

RECEIVED 06 October 2024
ACCEPTED 19 December 2024
PUBLISHED 22 January 2025

CITATION
Sun S and Yuan Z (2025) Cyclodextrin-assisted fluorescein decoration of gold nanoclusters for ratiometric and selective Hg^{2+} analysis.
Front. Anal. Sci. 4:1506786.
doi: 10.3389/frans.2024.1506786

Cyclodextrin-assisted fluorescein decoration of gold nanoclusters for ratiometric and selective Hg^{2+} analysis

Siyuan Sun and Zhiqin Yuan*

College of Chemistry, Beijing University of Chemical Technology, Beijing, China

Introduction: The construction of nanomaterial-based ratiometric detection systems usually requires covalent modification, which undergoes reactive environments and may change the natural properties of supporting nanomaterials.

Methods: In this study, dualemissive and fluorescein-decorated gold nanoclusters (F-Au NCs) through cyclodextrin-supported host–guest interaction (non-covalent modification) are explored as ratiometric Hg^{2+} nanoprobes through d^{10}–d^{10}-interactioncaused fluorescence quenching of Au NCs.

Results and Discussion: The fluorescein decoration only provides a fluorescent internal reference but does not change the Hg^{2+}-Au NCs affinity nature. Ratiometric and selective Hg^{2+} detection is achieved through the proposed F-Au NC probes with a limit of detection of 15 nM. The Hg^{2+} analysis in river water samples with small relative standard deviations validates the practical application of these probes.

KEYWORDS

ratiometric fluorescence, gold nanoclusters, Hg^{2+} detection, d^{10}-d^{10} interaction, host–guest interaction

Introduction

Ratiometric analysis with internal fluorescence reference has attracted growing attention due to its high sensitivity and accuracy (Huang et al., 2018; Park et al., 2020). Recently, the growth of nanoscience and nanotechnology has facilitated the development of versatile and functional nanomaterials for ratiometric analysis (Fu et al., 2022; Li et al., 2022; Li et al., 2017; Sun et al., 2023; Wu et al., 2024a; Wu et al., 2024b). For example, Zhang et al. (2022) reported the visualization of polymer–surfactant interaction with hyperbranched polyethyleneimine-encapsulated blue- and red-emitting gold nanoclusters (Au NCs). The linkage of fluorescent nanomaterials and fluorophores has permitted the construction of ratiometric detection systems for reactive oxygen species, small molecules, and metal ions (Duan et al., 2019; Liu et al., 2022; Wang et al., 2021; Wen et al., 2019; Wu et al., 2024b; Yang et al., 2020). These systems usually require covalent modification in reactive environments and may change the natural properties of supporting nanomaterials. The development of simple and effective modification strategies that do not require covalent bonds might benefit the construction of advanced nanomaterials.

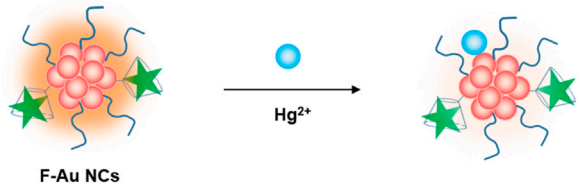

FIGURE 1
Schematic illustration of ratiometric Hg^{2+} detection with F-Au NC probes.

Noncovalent interactions, including hydrogen bonding, electrostatic attraction, π–π interaction, and hydrophobic affinity, have been widely applied for designing functional nanoarchitectures with diverse applications (Ghosh et al., 2023; Ju et al., 2024; Peluso and Chankvetadze, 2022; Rap et al., 2024), In particular, host–guest interaction occurs through various noncovalent forces, such as hydrogen bonding, van der Waals forces, or π–π stacking, resulting in the guest molecule being bound within a binding pocket of the host (Sayed and Pal, 2021; Yang et al., 2018; Zhu et al., 2023). Without the involvement of a covalent bond, it supports a dynamic noncovalent association between a host molecule and a guest molecule and has been extensively used for material fabrication. For instance, Fu et al. (2020) reported the construction of a bola-type supra-amphiphile with aggregation-induced emission characteristics by integrating host–guest interaction and topological self-assembly and applied it for mimicking light-harvesting antenna. In addition, the host–guest interaction also allows cavity binding, which may alter the chemical reactivity of guest molecules. As referred to in Eelkema's report, the transient host–guest complexation could regulate the enzymatic catalysis and control the hydrolysis of esters (van der Helm et al., 2022). Notice that the host–guest interaction does not change the chemical nature of substances; the combination of this specific interaction and target-responsive nanomaterials may permit the construction of ratiometric and selective detection systems with preserved recognition capability, which is theoretically feasible.

In recent decades, Au NC-based detection systems for metal ions, small molecules, DNA, RNA, and proteins have been widely explored because of their advantages of easy preparation, strong fluorescence, and tunable emission (Chen et al., 2015; Huang et al., 2007; Kurashige et al., 2016; Lu et al., 2020; Nasaruddin et al., 2018; Pyo et al., 2015; Shi et al., 2017; Yuan et al., 2017; Yuan et al., 2015; Yuan et al., 2011). As indicated in Duan et al. (2019) and Xie et al. (2010), Au NCs with surface Au(I) species are responsive to Hg^{2+} due to d^{10}–d^{10} interaction. However, sole intensity change might suffer interference from matrix and cause instable signals. It is thus speculated that Au NC-decoration with built-in fluorophore by host–guest interaction might endow ratiometric and accurate Hg^{2+} sensing. However, environment-sensitive characteristics make Au NCs variable during covalent functionalization, indicating that noncovalent modification is more proper for Au NC functionalization. In this study, we attempt to demonstrate our assumption by constructing a ratiometric Au NC-based sensing system by integrating host–guest interaction (typical noncovalent modification strategy). As a proof-of-concept, we propose fluorescein-functionalized Au NCs (F-Au NCs) for ratiometrically detecting Hg^{2+}. The decoration of fluorescein onto an Au NC surface was achieved by cyclodextrin (CD)-supported host–guest interaction. The addition of Hg^{2+} suppressed the orange emission of Au NCs, while the green emission of fluorescein only showed slight variation, leading to a ratiometric fluorescence response. The schematic illustration of Hg^{2+} detection using F-Au NCs probes is shown in Figure 1. The specificity of Hg^{2+}-caused ratiometric response of F-Au NC probes was investigated with other metal ions as possible interferents. The limit of detection (LOD) toward Hg^{2+} was found to be 15 nM (S/N = 3). Moreover, the practical application of proposed F-Au NC probes was verified by accurate Hg^{2+} analysis in river water samples. This strategy of using noncovalent modification-supported surface functionalization should be generalizable to the functionalization of a wide range of nanomaterials and the construction of ratiometric detection systems.

Methods

Materials, reagents, and instruments

Chloroauric acid tetrahydrate ($HAuCl_4.4H_2O$) was purchased from Damas-beta (Shanghai, China). Glutathione (GSH) was purchased from Shanghai Yuanye Bio-Technology Co. Ltd. (Shanghai, China). Mono-(6-mercapto-6-deoxy)-beta-cyclodextrin (β-CD-SH) was purchased from HWRK Chem. (Beijing, China). Potassium chloride (KCl), sodium chloride (NaCl), and sodium borohydride ($NaBH_4$) were purchased from Fuchen (Tianjin, China). Anhydrous calcium chloride ($CaCl_2$), hydrochloric acid (HCl), sodium hydroxide (NaOH), ethanol, and other chemicals were purchased from Beijing Chemical Reagent Company (Beijing, China). All chemicals used are analytical-reagent grade and used without further purification. All solutions were freshly prepared with deionized water (18.2 MΩ cm, Milli-Q, Millipore, Barnstead, CA, United States).

Transmission electron microscopy (TEM) images were collected with a HT7700 transmission electron microscope (Hitachi, Japan). UV–Vis absorption spectra were measured with a UV–3900H spectrophotometer (Shimadzu, Japan). Fluorescence spectra were obtained using an F-7000 fluorescence spectrophotometer (Hitachi, Japan). The pH values were measured with a benchtop pH meter (Orion plus, Thermo-Fisher, United States).

Synthesis of dual-emissive F-Au NCs

Dual-emissive F-Au NCs were prepared using a two-step strategy. First, CD-modified Au NCs (CD-Au NCs) were synthesized by a dual-ligand stabilization route based on our previous research with slight modification (Yang et al., 2018). Typically, freshly prepared $HAuCl_4$ (20 mM, 0.5 mL) and GSH (100 mM, 0.15 mL) were mixed, and 4.35 mL ultrapure water was added to make a 5.0-mL solution. The resultant mixture was stirred at 70°C for 24 h to yield GSH-capped Au NCs (GSH-Au NCs). Then, β-CD-SH was introduced into the solution, and the mixture was stirred at 50°C for 3 h to produce CD-Au NCs. The final concentration of β-CD-SH was 5 mM. The CD-Au NCs generated were filtered with a 10-KDa ultrafiltration tube (8,000 rpm, 10 min) to remove any unwanted thiol ligands and

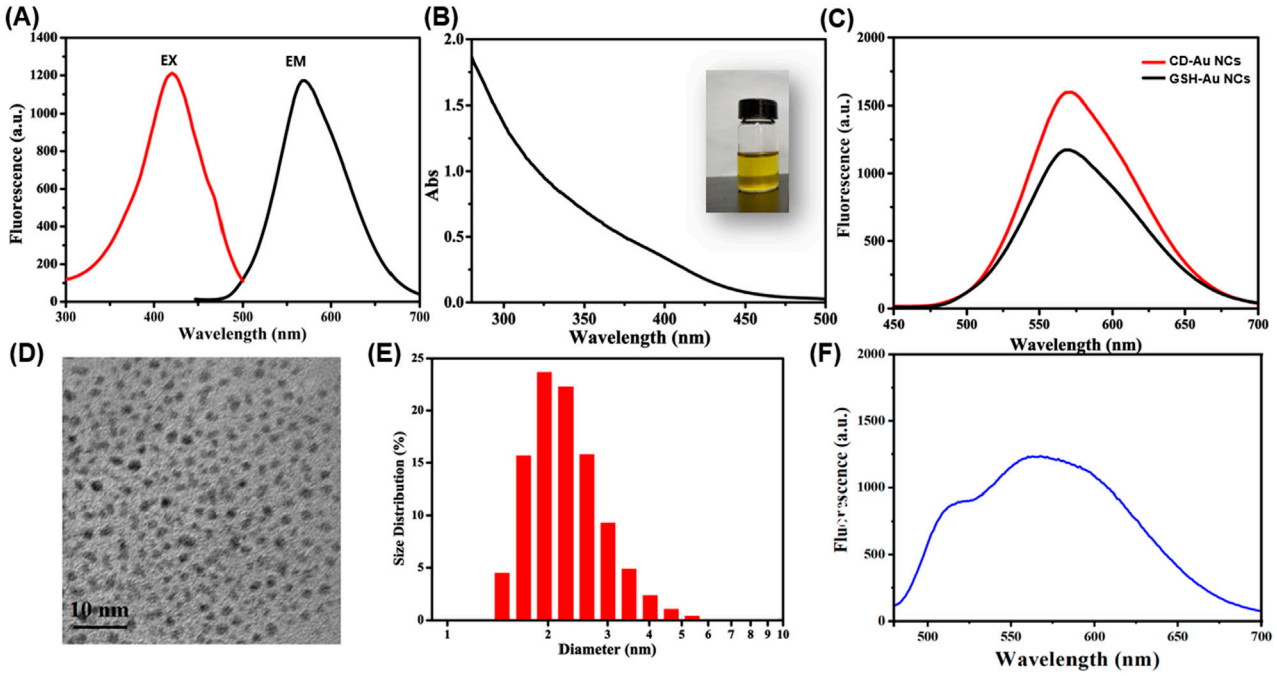

FIGURE 2
Fluorescence excitation and emission spectra **(A)** and UV–Vis absorption spectra **(B)** of CD-Au NCs. Inset image: photograph of CD-Au NCs solution under room light. **(C)** Fluorescence emission of GSH-Au NCs and CD-Au NCs. **(D)** TEM image of CD-Au NCs. **(E)** Statistic size distribution of CD-Au NCs. **(F)** Fluorescence emission of dual-emissive F-Au NCs.

reactants. To prepare F-Au NCs, 30-mL CD-Au NC solution was mixed with 300 μL fluorescein (final concentration: 300 nM). After 2 h shaking at 30°C, the mixture was filtered with a 10-KDa ultrafiltration tube (8,000 rpm, 10 min) and dispersed in 10.0 mL solution and then stored at 4°C before use. The concentration of F-Au NCs was determined to be 0.25 mg/mL.

Sensitivity and selectivity measurement

For sensitivity evaluation, a serial of Hg^{2+} stock solutions were prepared. In Hg^{2+} detection assays, 750 μL ultrapure water was added into a 1.5-mL centrifuge tube containing 100 μL PB buffer (pH 7.4) and 100 μL F-Au NCs probes, and then 50 μL Hg^{2+} solution with various concentrations was added to make the final volume of 1 mL. After 5-min reaction at room temperature, the fluorescence emission spectra were collected by a F-7000 fluorescence spectrophotometer. For selectivity tests, 750 μL ultrapure water was added into a 1.5-mL centrifuge tube containing 100 μL PB buffer (pH 7.4) and 100 μL F-Au NC probes, and then 50 μL metal ion solution was added to make the final volume of 1 mL. The final concentration of all metal ions was 5.0 μM. After 5-min reaction at room temperature, the fluorescence emission spectra were collected by an F-7000 fluorescence spectrophotometer. For anti-interference assays, 700 μL ultrapure water was added into a 1.5-mL centrifuge tube containing 100 μL PB buffer and 100 μL F-Au NCs probes, and then 50 μL metal ion solution and 50 μL Hg^{2+} solution were added to make the final volume of 1 mL. After 5-min reaction at room temperature, the fluorescence emission spectra were collected by an F-7000 fluorescence spectrophotometer.

River water sample analysis

River water samples were obtained from the local Xiaoyue River in Yuandadu Park. The water samples obtained were first passed through a filter membrane with a pore size of 0.22 μm and were then ultrafiltered with a 3-KDa ultrafiltration tube to remove large aggregates or particles. To detect Hg^{2+} content, an 800-μL water sample was added into a 1.5-mL centrifuge tube containing 100 μL PB buffer (pH 7.4) and 100 μL F-Au NC probes to make the final volume of 1 mL. After 5-min reaction at room temperature, the fluorescence emission spectra were collected by an F-7000 fluorescence spectrophotometer. To conduct standard addition experiments, a 750-μL water sample was added to a 1.5-mL centrifuge tube containing 100 μL PB buffer (pH 7.4) and 100 μL F-Au NC probes, and then 50 μL Hg^{2+} solution was added to make the final volume of 1 mL. The final concentrations of added Hg^{2+} were 5.0 μM, 10.0 μM, and 15.0 μM. After 5-min reaction at room temperature, the fluorescence emission spectra were collected by an F-7000 fluorescence spectrophotometer.

Results and discussion

Synthesis and characterization of F-Au NCs

At the start, the dual-emissive F-Au NCs were synthesized based on a two-step protocol. That is, CD-Au NCs were first prepared, and the F-Au NCs were obtained after fluorescein decoration. As shown in Figure 2A, the maxima fluorescence

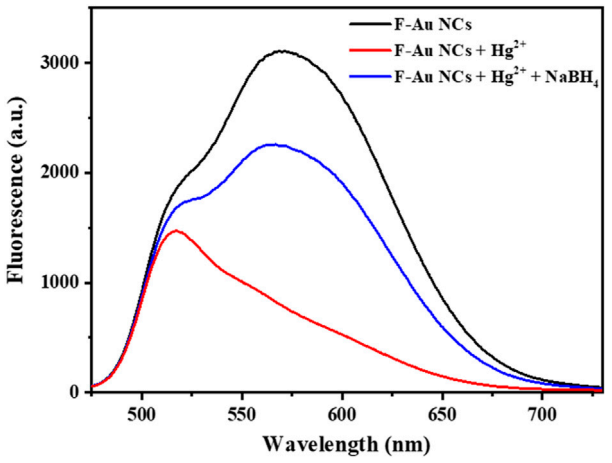

FIGURE 3
Fluorescence emission spectra of F-Au NCs without (black line) and with (red line) the addition of Hg^{2+} in the absence and presence (blue line) of $NaBH_4$.

excitation and emission wavelengths of CD-Au NCs were found at 421 nm and 570 nm, respectively. The fluorescence excitation and emission spectra were consistent with Yang et al. (2018). In addition, the UV–Vis absorption spectrum of CD-Au NCs showed a broad absorbance band at approximately 300–450 nm (Figure 2B). In comparison with GSH-Au NCs, CD-Au NCs showed stronger fluorescence without a change in the emission profile (Figure 2C). The fluorescence increment might be attributed to the CD modification-mediated increase of surface thiolate ligand density and the diminution the nonradiative transition. The TEM image indicates that the CD-Au NCs were spherical, with an average size of 2.4 ± 0.2 nm (Figures 2D, E). These results suggest the generation of CD-Au NCs. After fluorescein decoration, a new emission band centered at 514 nm was observed (Figure 2F), while the emission band centered at 567 nm was preserved, revealing the successful preparation of dual-emissive F-Au NCs.

Hg^{2+}-induced ratiometric fluorescence variation

To investigate the fluorescence response of dual-emissive F-Au NCs toward Hg^{2+}, the fluorescence emission spectra of F-Au NCs were obtained before and after the addition of Hg^{2+}. As shown in Figure 3, the orange emission centered at 567 nm displayed a dramatic decrement (~75%) during the introduction of Hg^{2+}, indicating that Hg^{2+} can cause the fluorescence quenching of Au NCs. However, the green emission centered at 514 nm showed no distinct variation. The maintained green emission might act as an internal fluorescence reference for Hg^{2+} recognition. The emission profile of Au NCs showed no visible change with the addition of Hg^{2+}, suggesting that the fluorescence quenching is not assigned to the generation of new Au NCs with different structure. It is well-known that Hg^{2+} can strongly bind to Au^{+} through d^{10}–d^{10} interaction, which alters the electron transition and quenches the fluorescence of Au NCs (Xie et al., 2010). In general, partial Au(I) exists on the surface of thiolate-stabilized Au NCs, which is important for the emission character of Au NCs (Wang et al., 2023; Yuan et al., 2013). To understand the d^{10}–d^{10}-mediated Hg^{2+}-Au^{+} interaction-induced fluorescence quenching, a strong reducing agent ($NaBH_4$) was introduced into the Hg^{2+}-F-Au NC mixture. Interestingly, the fluorescence at approximately 567 nm showed visible recovery after the addition of $NaBH_4$. The recovered orange emission indicated that the Hg^{2+}-induced fluorescence variation can be attributed to the Hg^{2+}-Au^{+} d^{10}–d^{10} interaction-supported fluorescence quenching of Au NCs. Additionally, we found that fluorescein emits strong green light compared to F-Au NCs, while the introduction of Hg^{2+} only caused the quenching of orange emission but did not enhance the green emission of adsorbed fluorescein. It can be seen that the UV–Vis absorption spectra of Au NCs displayed an overlap in the emission profile of fluorescein, leading to fluorescence resonance energy transfer between fluorescein and Au NCs. Despite the Hg^{2+}-induced fluorescence quenching of Au NCs, the absorption character of Au NCs was not affected. Therefore, the fluorescence resonance energy transfer process was not suppressed, leading to the unchanged green emission. Hg^{2+}-F-Au NC binding not only suppresses the orange emission of Au NCs through strong d^{10}–d^{10} interaction but also maintains the green emission of fluorescein by reserving the fluorescence resonance energy transfer pathway, which endows a ratiometric and sensitive fluorescence response toward Hg^{2+}.

Hg^{2+} sensing in aqueous media

Since the introduction of Hg^{2+} into dual-emissive F-Au NC solution caused ratiometric fluorescence variation, such a response might be able to be utilized for fluorometric Hg^{2+} detection by using F-Au NCs as the fluorescence reporters. Since fluorescein decoration is important to ratiometric variation, the fluorescein dosage was optimized to achieve sensitive Hg^{2+} detection. As shown in Figure 4A, the relative fluorescence ratio variation was monitored under different fluorescein dosage using R ($R = (I_{514}/I_{567})/(I_{514}/I_{567})_0$) as the reporting signal. It can be seen that the R value showed an increment with the increasing fluorescein concentration from 100 to 300 nM. However, it showed reverse trends when the fluorescein concentration was higher than 300 nM. A possible reason for this phenomenon is that the low fluorescein concentration cannot support effective green emission due to the fluorescence resonance energy transfer and thus shows a small R value only. However, ultrahigh fluorescein concentration contributes strong green emission and a large value of $(I_{514}/I_{567})_0$. As a result, only a small R value is obtained with ultrahigh fluorescein concentration. In this case, 300 nM fluorescein was used for the decoration of Au NCs. In addition, the solution pH is also important to Hg^{2+} sensing. The fluorescein only shows strong emission under alkaline conditions, with only weak emission in an acidic environment. In addition, a Hg^{2+} dismutation reaction occurs in acidic conditions and forms $Hg(OH)_2$ in alkaline solution. Those pH-dependent factors

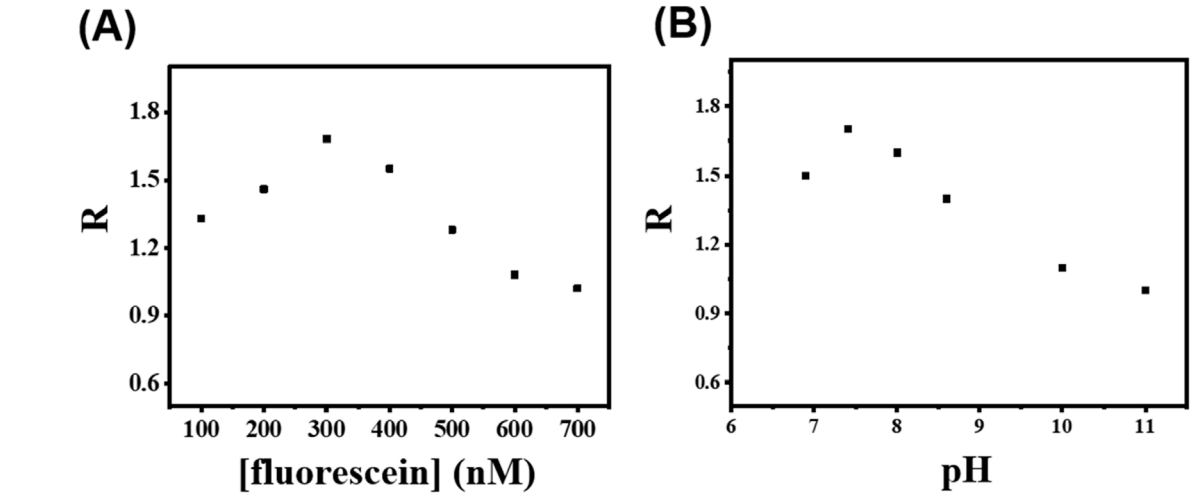

FIGURE 4
Optimization of Hg^{2+}-sensing parameters. Fluorescence intensity ratio variation R (R = $(I_{514}/I_{567})/(I_{514}/I_{567})_0$) of F-Au NC solution with the addition of Hg^{2+} *versus* fluorescein decoration concentration **(A)** and reaction pH value **(B)**.

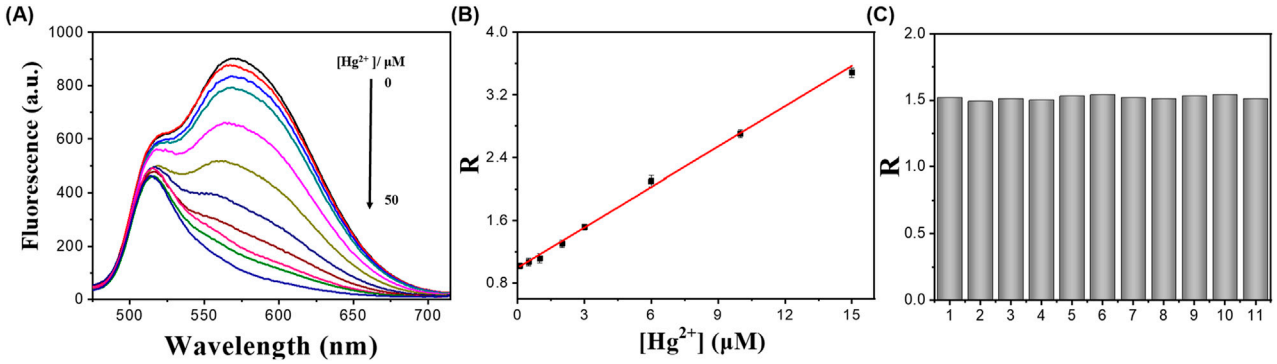

FIGURE 5
(A) Fluorescence emission spectra of F-Au NC solution upon adding Hg^{2+} with various concentrations. **(B)** Plots of fluorescence intensity ratio variation R (R = $(I_{514}/I_{567})/(I_{514}/I_{567})_0$) of F-Au NC solution *versus* Hg^{2+} concentrations. **(C)** Fluorescence intensity ratio variation R of 11 repeated measurements of F-Au NC solution toward 3.0 μM Hg^{2+}.

TABLE 1 Hg^{2+} analysis in Xiaoyue River water and tap water samples with the proposed F-Au NC probes.

Sample	Spiked Hg^{2+} (μM)	Found (μM)	Recovery (%)	RSD (%, n = 5)
River water	0.5	0.5 ± 0.1	100.0	2.6
	5.0	5.1 ± 0.1	102.0	1.8
	10.0	9.9 ± 0.2	99.0	2.4
	15.0	15.2 ± 0.2	101.3	2.1
Tap water	0.5	0.5 ± 0.1	100.0	2.8
	5.0	4.9 ± 0.1	98.0	2.1
	10.0	10.1 ± 0.3	101.0	2.3
	15.0	15.1 ± 0.2	100.7	2.4

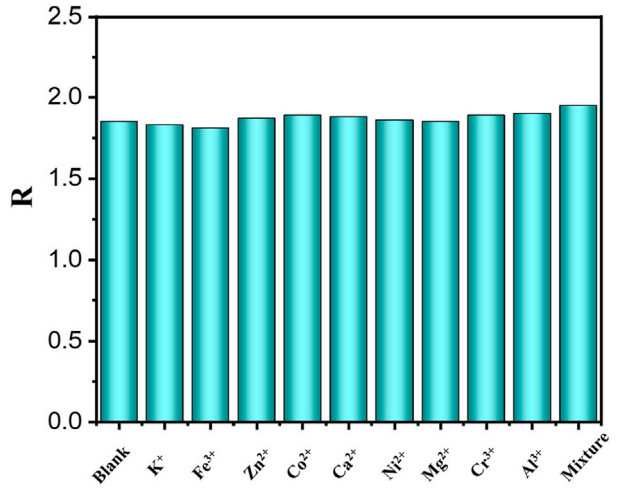

FIGURE 6
Fluorescence intensity ratio variation R ($R = (I_{514}/I_{567})/(I_{514}/I_{567})_0$) of F-Au NCs upon adding various metal ions in the presence of Hg^{2+}.

can influence Hg^{2+} detection sensitivity. It was seen that the maximum R value occurred under pH 7.4 (Figure 4B), so the following experiments were conducted at pH 7.4 without further pH adjustment.

The sensitivity evaluation toward Hg^{2+}-sensing with F-Au NCs was first investigated based on ratiometric analysis. The fluorescence emission spectra of F-Au NC solution were recorded after the addition of Hg^{2+} with various concentrations. As shown in Figure 5A, the orange fluorescence (567 nm) of Au NCs gradually decreased with the increasing Hg^{2+} concentration without change of spectral shape. The maintained emission profile forms a Hg^{2+}-F-Au NC complex rather than producing new Au NC components. Meanwhile, the green fluorescence was unchanged, resulting in the increased fluorescence intensity ratio of I_{514}/I_{567}. Using the R value as the reporting signal, a linear response relation was found with the Hg^{2+} concentration range from 0.1 to 15.0 μM. As manifested in Figure 5B, the R-value plots could be described with the linear equation $y = 0.995 + K[Q]$ ($R^2 = 0.996$), where y is the R value, K is the corresponding fluorescence response constant, and [Q] is the Hg^{2+} concentration. Throughout the linear regression treatment, the fluorescence response constant K was calculated to be $1.72 \times 10^5\ M^{-1}$. The reproducibility of Hg^{2+} sensing was also investigated by ten repeated measurements of the Hg^{2+}-induced fluorescence response of F-Au NCs. As displayed in Figure 5C, with 11 repeated measurements of 3.0 μM Hg^{2+}-induced fluorescence changes, only a slight variation was observed in the R value, and a low relative standard deviation (RSD) value of 1.6% was obtained, suggesting the high reproducibility of proposed F-Au NC probes. The LOD toward Hg^{2+} by F-Au NC probes was determined to be 15 nM (S/N = 3). This LOD is comparable to many reported Hg^{2+} detection methods (Bharati Jaryal et al., 2024; Luo et al., 2021; Musikavanhu et al., 2024; Zhao et al., 2024).

To evaluate the proposed F-Au NCs probes, the selectivity assessment is important. To understand whether the Hg^{2+}-induced ratiometric fluorescence change is specific, the fluorescence emission spectra of F-Au NC probes in the presence of Hg^{2+} and other possible interferents were measured. In this study, metal ions including K^+, Ca^{2+}, Fe^{3+}, Co^{2+}, Ni^{2+}, Zn^{2+}, Mg^{2+}, Cr^{3+}, and Al^{3+} were chosen for the specificity evaluation. The concentrations of Hg^{2+} and other metal ions were set at 5 μM. None of these metal ions could cause a comparable increment of R value as did Hg^{2+}, indicating that the Hg^{2+}-induced ratiometric variation of F-Au NC probes is selective. The Hg^{2+}-induced ratiometric variation was not affected by the co-existence of various metal ions (Figure 6), even with the mixture of metal ions, further demonstrating the high specificity of Hg^{2+} detection with F-Au NC probes. The satisfying selectivity is largely ascribed to the strong Hg^{2+}-Au^+ d^{10}–d^{10} interaction. Taken together, the F-Au NC probes enabled selective and reproducible Hg^{2+} detection, with comparable sensing performances compared to other reported probes.

Hg^{2+} analysis in river water and tap water samples

The favorable sensitivity and selectivity of F-Au NC probes suggest the possibility of Hg^{2+} analysis in real samples. In this study, the practical application of F-Au NC probes was verified by Hg^{2+} analysis in river- and tap-water samples. The collected river- or tap-water samples were first centrifuged-filtered to remove large aggregates. The Hg^{2+}-induced signal variation was not detected in the river- or tap-water samples, indicating that the Hg^{2+} contents in both river- and tap-water were lower than the LOD of Au NC probes. Accuracy was validated using standard addition protocols. As shown in Table 1, the detected Hg^{2+} contents were generally consistent with those added, with recovery values close to 100% (98.0–102.0%). The RSD values were also small (≦ 2.8%, n = 5), further revealing the high accuracy of the proposed F-Au NC probes. It can be concluded that the proposed dual-emissive F-Au NC-based ratiometric system is applicable for Hg^{2+} detection in real water samples.

Conclusion

We established a ratiometric Hg^{2+} detection platform based on dual-emissive F-Au NC probes. The CD-assisted fluorescein modification replies on host–guest interaction and does not change the reactivity of Au NCs. By integrating the Hg^{2+}-Au^+ d^1--d^{10} interaction-mediated fluorescence quenching of Au NCs and fluorescein internal reference, the proposed platform enables a ratiometric and selective response toward Hg^{2+} over other metal ions. On the basis of F-Au NC probes, rapid Hg^{2+} perception with an LOD of 15 nM is achieved under optimized conditions. Practical application is also validated by accurate Hg^{2+} analysis in river-water samples. This study not only reports a ratiometric Hg^{2+} detection system but also demonstrates the preparation of functional Au NCs by utilizing host–guest interaction. Thus, the development of versatile Au NCs with designed functions for expected applications is possible by involving noncovalent modification.

Data availability statement

The raw data supporting the conclusions of this article will be made available by the authors, without undue reservation.

Author contributions

SS: formal analysis, investigation, methodology, and writing–original draft. ZY: conceptualization, funding acquisition, supervision, validation, visualization, writing–original draft, and writing–review and editing.

Funding

The authors declare that financial support was received for the research, authorship, and/or publication of this article. This work was supported by the National Natural Science Foundation of China (22074005) and the Natural Science Foundation of Beijing Municipality (2202038).

Conflict of interest

The authors declare that the research was conducted in the absence of any commercial or financial relationships that could be construed as a potential conflict of interest.

Generative AI statement

The authors declare that no generative AI was used in the creation of this manuscript.

Publisher's note

References

Bharati Jaryal, V., Singh, R., Ali, S., Bououdina, M., and Gupta, N. (2024). Fabrication of a reversible fluorescence sensor based on nitrogen-sulfur Co-doped multiwalled carbon nanotubes for detection of mercury ions: experimental and DFT insights. *ChemistrySelect* 9 (36), e202400699. doi:10.1002/slct.202400699

Chen, L.-Y., Wang, C.-W., Yuan, Z., and Chang, H.-T. (2015). Fluorescent gold nanoclusters: recent advances in sensing and imaging. *Anal. Chem.* 87 (1), 216–229. doi:10.1021/ac503636j

Duan, B., Wang, M., Li, Y., Jiang, S., Liu, Y., and Huang, Z. (2019). Dual-emitting zein-protected gold nanoclusters for ratiometric fluorescence detection of Hg^{2+}/Ag^{+} ions in both aqueous solution and self-assembled protein film. *New J. Chem.* 43 (37), 14678–14683. doi:10.1039/C9NJ03524A

Fu, L., Chen, Q., and Jia, L. (2022). Carbon dots and gold nanoclusters assisted construction of a ratiometric fluorescent biosensor for detection of Gram-negative bacteria. *Food Chem.* 374, 131750. doi:10.1016/j.foodchem.2021.131750

Fu, S., Su, X., Li, M., Song, S., Wang, L., Wang, D., et al. (2020). Controllable and diversiform topological morphologies of self-assembling supra-amphiphiles with aggregation-induced emission characteristics for mimicking light-harvesting antenna. *Adv. Sci.* 7 (20), 2001909. doi:10.1002/advs.202001909

Ghosh, S., Changotra, A., Petrone, D. A., Isomura, M., Carreira, E. M., and Sunoj, R. B. (2023). Role of noncovalent interactions in inducing high enantioselectivity in an alcohol reductive deoxygenation reaction involving a planar carbocationic intermediate. *J. Am. Chem. Soc.* 145 (5), 2884–2900. doi:10.1021/jacs.2c10975

Huang, C.-C., Yang, Z., Lee, K.-H., and Chang, H.-T. (2007). Synthesis of highly fluorescent gold nanoparticles for sensing mercury(II). *Angew. Chem. Int. Ed.* 46 (36), 6824–6828. doi:10.1002/anie.200700803

Huang, X., Song, J., Yung, B. C., Huang, X., Xiong, Y., and Chen, X. (2018). Ratiometric optical nanoprobes enable accurate molecular detection and imaging. *Chem. Soc. Rev.* 47 (8), 2873–2920. doi:10.1039/C7CS00612H

Ju, H., Wang, B., Li, M., Hao, J., Si, W., Song, S., et al. (2024). Tracking noncovalent interactions of π, π-hole, and ion in molecular complexes at the single-molecule level. *J. Am. Chem. Soc.* 146 (36), 25290–25298. doi:10.1021/jacs.4c09504

Kurashige, W., Niihori, Y., Sharma, S., and Negishi, Y. (2016). Precise synthesis, functionalization and application of thiolate-protected gold clusters. *Coord. Chem. Rev.* 320-321, 238–250. doi:10.1016/j.ccr.2016.02.013

Li, S., Ma, Q., Wang, C., Yang, K., Hong, Z., Chen, Q., et al. (2022). Near-infrared II gold nanocluster assemblies with improved luminescence and biofate for *in vivo* ratiometric imaging of H_2S. *Anal. Chem.* 94 (5), 2641–2647. doi:10.1021/acs.analchem.1c05154

Li, Z., Guo, S., Yuan, Z., and Lu, C. (2017). Carbon quantum dot-gold nanocluster nanosatellite for ratiometric fluorescence probe and imaging for hydrogen peroxide in living cells. *Sens. Actuators, B* 241, 821–827. doi:10.1016/j.snb.2016.10.134

Liu, Y., Liu, Y., Zhang, J., Zheng, J., Yuan, Z., and Lu, C. (2022). Catechin-inspired gold nanocluster nanoprobe for selective and ratiometric dopamine detection via forming azamonardine. *Spectrochimica Acta Part A Mol. Biomol. Spectrosc.* 274, 121142. doi:10.1016/j.saa.2022.121142

Lu, F., Yang, H., Tang, Y., Yu, C.-J., Wang, G., Yuan, Z., et al. (2020). 11-Mercaptoundecanoic acid capped gold nanoclusters with unusual aggregation-enhanced emission for selective fluorometric hydrogen sulfide determination. *Microchim. Acta* 187 (4), 200. doi:10.1007/s00604-020-4159-1

Luo, Q., Huang, Y., Lei, Z., Peng, J., Xu, D., Guo, X., et al. (2021). Wood-derived nanocellulose hydrogel incorporating gold nanoclusters using *in situ* multistep reactions for efficient sorption and sensitive detection of mercury ion. *Industrial Crops Prod.* 173, 114142. doi:10.1016/j.indcrop.2021.114142

Musikavanhu, B., Huang, X., Ma, Q., Xue, Z., Feng, L., and Zhao, L. (2024). Rhodamine-benzothiazole-thiophene: a triangular molecular tool for simultaneous detection of Hg^{2+} and Cu^{2+}. *Microchem. J.* 206, 111549. doi:10.1016/j.microc.2024.111549

Nasaruddin, R. R., Chen, T., Yan, N., and Xie, J. (2018). Roles of thiolate ligands in the synthesis, properties and catalytic application of gold nanoclusters. *Coord. Chem. Rev.* 368, 60–79. doi:10.1016/j.ccr.2018.04.016

Park, S.-H., Kwon, N., Lee, J.-H., Yoon, J., and Shin, I. (2020). Synthetic ratiometric fluorescent probes for detection of ions. *Chem. Soc. Rev.* 49 (1), 143–179. doi:10.1039/C9CS00243J

Peluso, P., and Chankvetadze, B. (2022). Recognition in the domain of molecular chirality: from noncovalent interactions to separation of enantiomers. *Chem. Rev.* 122 (16), 13235–13400. doi:10.1021/acs.chemrev.1c00846

Pyo, K., Thanthirige, V. D., Kwak, K., Pandurangan, P., Ramakrishna, G., and Lee, D. (2015). Ultrabright luminescence from gold nanoclusters: rigidifying the Au(I)–Thiolate shell. *J. Am. Chem. Soc.* 137 (25), 8244–8250. doi:10.1021/jacs.5b04210

Rap, D. B., Schrauwen, J. G. M., Redlich, B., and Brünken, S. (2024). Noncovalent interactions steer the formation of polycyclic aromatic hydrocarbons. *J. Am. Chem. Soc.* 146 (33), 23022–23033. doi:10.1021/jacs.4c03395

Sayed, M., and Pal, H. (2021). An overview from simple host–guest systems to progressively complex supramolecular assemblies. *Phys. Chem. Chem. Phys.* 23 (46), 26085–26107. doi:10.1039/D1CP03556H

Shi, L., Zhu, L., Guo, J., Zhang, L., Shi, Y., Zhang, Y., et al. (2017). Self-assembly of chiral gold clusters into crystalline nanocubes of exceptional optical activity. *Angew. Chem. Int. Ed.* 56 (48), 15397–15401. doi:10.1002/anie.201709827

Sun, Y., Zhou, Z., Peng, P., Shu, T., Su, L., and Zhang, X. (2023). Protein-directed Au(0)-rich gold nanoclusters as ratiometric luminescence sensors for auric ions via comproportionation-induced emission enhancement. *Anal. Chem.* 95 (14), 5886–5893. doi:10.1021/acs.analchem.2c04718

van der Helm, M. P., Li, G., Hartono, M., and Eelkema, R. (2022). Transient host–guest complexation to control catalytic activity. *J. Am. Chem. Soc.* 144 (21), 9465–9471. doi:10.1021/jacs.2c02695

Wang, D., Gao, X., Jia, J., Zhang, B., and Zou, G. (2023). Valence-State-engineered electrochemiluminescence from Au nanoclusters. *ACS Nano* 17 (1), 355–362. doi:10.1021/acsnano.2c08474

Wang, M., Chen, J., Jiang, S., Nie, Y., and Su, X. (2021). Rapid synthesis of dual proteins co-functionalized gold nanoclusters for ratiometric fluorescence sensing of polynucleotide kinase activity. *Sens. Actuators, B* 329, 129200. doi:10.1016/j.snb.2020.129200

Wen, Z., Song, S., Hu, T., Wang, C., Qu, F., Wang, P., et al. (2019). A dual emission nanocomposite prepared from copper nanoclusters and carbon dots as a ratiometric fluorescent probe for sulfide and gaseous H_2S. *Microchim. Acta* 186 (4), 258. doi:10.1007/s00604-019-3295-y

Wu, H., Wang, Q., Dong, M., Liu, X., and Tang, Y. (2024a). pH-responsive dual-emission carbon dots for the ratiometric detection of organophosphorus pesticides in Brassica chinensis and Hg^{2+} in water. *Food Chem.* 454, 139755. doi:10.1016/j.foodchem.2024.139755

Wu, Y., Sun, L.-L., Han, H.-H., He, X.-P., Cao, W., and James, T. D. (2024b). Selective FRET nano probe based on carbon dots and naphthalimide–isatin for the ratiometric detection of peroxynitrite in drug-induced liver injury. *Chem. Sci.* 15 (2), 757–764. doi:10.1039/D3SC05010F

Xie, J., Zheng, Y., and Ying, J. Y. (2010). Highly selective and ultrasensitive detection of Hg2+ based on fluorescence quenching of Au nanoclusters by Hg2+–Au+ interactions. *Chem. Commun.* 46 (6), 961–963. doi:10.1039/B920748A

Yang, H., Lu, F., Sun, Y., Yuan, Z., and Lu, C. (2018). Fluorescent gold nanocluster-based sensor array for nitrophenol isomer discrimination via an integration of host–guest interaction and inner filter effect. *Anal. Chem.* 90 (21), 12846–12853. doi:10.1021/acs.analchem.8b03394

Yang, H., Yang, Y., Liu, S., Zhan, X., Zhou, H., Li, X., et al. (2020). Ratiometric and sensitive cyanide sensing using dual-emissive gold nanoclusters. *Anal. Bioanal. Chem.* 412 (23), 5819–5826. doi:10.1007/s00216-020-02806-2

Yuan, Z., Du, Y., and He, Y. (2017). Hyperbranched polyamine assisted synthesis of dual-luminescent gold composite with pH responsive character. *Methods Appl. Fluoresc.* 5 (1), 014011. doi:10.1088/2050-6120/aa625d

Yuan, Z., Du, Y., Tseng, Y.-T., Peng, M., Cai, N., He, Y., et al. (2015). Fluorescent gold nanodots based sensor array for proteins discrimination. *Anal. Chem.* 87 (8), 4253–4259. doi:10.1021/ac5045302

Yuan, Z., Peng, M., He, Y., and Yeung, E. S. (2011). Functionalized fluorescent gold nanodots: synthesis and application for Pb^{2+} sensing. *Chem. Commun.* 47 (43), 11981–11983. doi:10.1039/c1cc14872a

Yuan, Z., Peng, M., Shi, L., Du, Y., Cai, N., He, Y., et al. (2013). Disassembly mediated fluorescence recovery of gold nanodots for selective sulfide sensing. *Nanoscale* 5 (11), 4683–4686. doi:10.1039/c2nr33202g

Zhang, J., Liu, Y., Liu, Y., Liu, W., Lu, F., Yuan, Z., et al. (2022). Gold nanocluster-encapsulated hyperbranched polyethyleneimine for selective and ratiometric dopamine analyses by enhanced self-polymerization. *Front. Chem.* 10, 928607. doi:10.3389/fchem.2022.928607

Zhao, C., Aziz, A., Lu, W., Xu, H., Asif, M., Shuang, S., et al. (2024). A turn-on anthraquinone-derived colorimetric and fluorometric dual-mode probe for highly selective Hg^{2+} determination and bioimaging in living organisms. *J. Hazard. Mat.* 479, 135694. doi:10.1016/j.jhazmat.2024.135694

Zhu, H., Chen, L., Sun, B., Wang, M., Li, H., Stoddart, J. F., et al. (2023). Applications of macrocycle-based solid-state host–guest chemistry. *Nat. Rev. Chem.* 7 (11), 768–782. doi:10.1038/s41570-023-00531-9